High Energy Density Simulations for Inertial Fusion Energy Reactor Design

G.A. Moses and J.F. Santarius

September 2004

UWFDM-1258

Presented at the 16th ANS Topical Meeting on Fusion Energy, 14–16 September 2004, Madison WI.

FUSION TECHNOLOGY INSTITUTE

UNIVERSITY OF WISCONSIN

MADISON WISCONSIN

High Energy Density Simulations for Inertial Fusion Energy Reactor Design

G.A. Moses and J.F. Santarius

Fusion Technology Institute
University of Wisconsin
1500 Engineering Drive
Madison, WI 53706

http://fti.neep.wisc.edu

September 2004

UWFDM-1258

Presented at the 16th ANS Topical Meeting on Fusion Energy, 14–16 September 2004, Madison WI.

HIGH ENERGY DENSITY SIMULATIONS FOR INERTIAL FUSION ENERGY REACTOR DESIGN

Gregory A. Moses and John F. Santarius

Fusion Technology Institute, University of Wisconsin-Madison:
1500 Engineering Drive, Madison, Wisconsin, 53706,
moses@engr.wisc.edu and santarius@engr.wisc.edu

The so-called "threat spectra" of an inertial fusion energy (IFE) high gain target (neutron, x-ray, and ion energy fraction and particle spectra) are the usual starting point for IFE reactor conceptual design. The threat spectra are typically computed using the same radiation hydrodynamics and thermonuclear burn computer simulation codes used to compute implosion, ignition and burn. We analyze the validity of this model for simulating the expansion of the direct drive IFE target plasma and for computing threat spectra. Particular attention is paid to the collisionality of the expanding plasma.

I. INTRODUCTION

The promise of inertial fusion as an energy source for electric power generation is elucidated in conceptual reactor design studies. These studies use the best available experimental information to predict the fusion performance and performance of the other reactor features such as materials strength, radiation damage, tritium breeding, heat transfer, etc. For those properties where experimental evidence is not available, computer simulations are often used. One aspect where computer simulations are predominantly relied upon are the high energy density radiation hydrodynamics simulations of target burn and expansion and the reactor cavity and first wall response to the energetic target constituents (x-rays, ions, and neutrons).[1]

Simulations of target implosion and ignition are of course a well developed discipline and are a cornerstone of the U.S.D.O.E. inertial confinement fusion program and other programs worldwide. The post-ignition target performance and subsequent target expansion are less well studied and are the subject of this paper. The starting point is the same radiation hydrodynamics model used to simulate target implosion and burn. The questions addressed are:

What are the fundamental characteristics of post-burn target expansion?

Is a fluid-based model adequate to simulate high gain target expansion in a vacuum?

II. THREAT SPECTRA

The energetic target constituents (neutrons, x-rays, and ions) created during the thermonuclear burn are called the threat spectra. The threat spectra are typically computed using a radiation hydrodynamics model. Detailed neutron transport methods such as discrete ordinates are used to solve the linear neutron transport equation and predict the neutron spectrum emerging from the outer boundary of the expanding post-burn target plasma. Likewise, the x-ray spectrum emerging from the expanding target plasma is computed as part of the non-linear radiation hydrodynamics simulation. The x-ray transport might be computed using flux-limited multi-group diffusion or a number of other transport methods. The plasma only emits x-rays while it is hot and the expanding plasma quickly cools to temperatures below which x-ray emission becomes unimportant. Thus the neutrons and x-rays are emitted from the plasma over a relatively short time period following burn. The transport methods used to compute these spectra are valid over the range of plasma density encountered in the simulation.

The ion spectrum is comprised of the ionic constituents of the expanding plasma. Here the radiation hydrodynamic model must be carefully assessed. Fundamental to this model is the fluid approximation to the plasma behavior. While the plasma is imploded and burns, this collisional fluid model accurately simulates the behavior of the plasma. However, during the post-burn expansion phase, the spherical plasma collisionality varies greatly from its center to its outer boundary. This variation deserves a more careful analysis. The typical analysis simulates the post-burn target expansion to a time when the plasma temperature reaches very low values due to expansion cooling and the plasma energy is found in the outward kinetic energy of the fluid. Hydrodynamics simulations predict that this kinetic energy varies spatially with radius, increasing with radius. This kinetic energy is assigned to individual ions as they reside at different radii at the time the simulation stops and thus the ion spectrum is obtained. A cruder zero-dimensional estimate is to run the simulation until temperatures are low, x-ray emission is low and all energy is in plasma kinetic energy. Ignore

the spatial variation of ionic species and assign this total kinetic energy per atomic mass unit (AMU) for all of the AMU's in the plasma. In this case, the energy per ion is proportional to the ion mass. While seemingly a less accurate estimate, this has the advantage of not "over-interpreting" the spatial profile results predicted by the hydrodynamics simulation when those results might be based upon invalid collisionality regimes.

II.A. High Gain Target Dynamics

The configuration of a particular direct drive high gain target is shown in Fig. 1. This target is chosen because we have a well-characterized 1-D radiation hydrodynamic simulation of its implosion and burn using the BUCKY code.[2] While this is only one target design, the conclusions of this paper are valid for direct drive targets similar to the one studied here. The conclusions are not necessarily valid for the expansion of indirect drive targets where a substantial mass is included in the surrounding hohlraum.

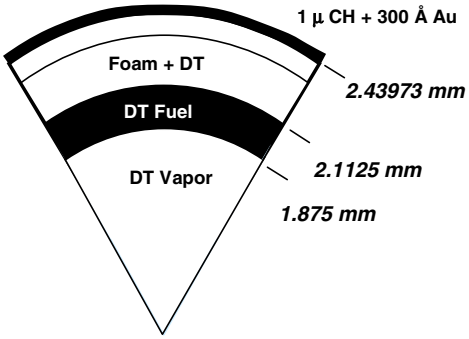

Fig. 1. Reference direct-drive ICF target.

Ignition is defined as the time during which almost all of the neutrons get generated. The cumulative neutron production appears in Fig. 2. The rapid generation of high pressure at the center of the target during thermonuclear burn then launches a spherically expanding shock wave into the spherically expanding plasma. This is seen in the r-t plot shown in Fig. 3.

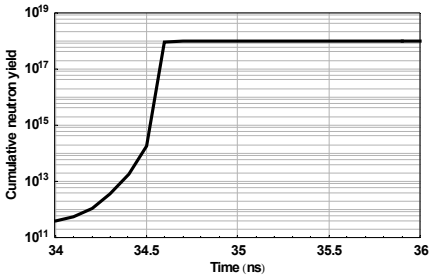

Fig. 2. Neutron production near the time of ignition.

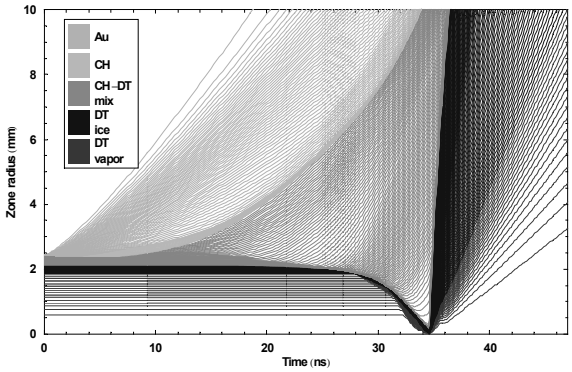

Fig. 3. Lagrangian zone radii vs. time for the reference case.

Ignition for the reference case occurs approximately from 34.5-34.6 ns. The mass density, temperature, velocity profiles, and charge state vs. radius of the reference target near ignition are shown in Fig. 4, Fig. 5, Fig. 6, and Fig. 7, where each dot characterizes a Lagrangian zone of constant mass. The density varies from ~4000 g/cm^3 in the compressed DT fuel to ~10^{-7} g/cm^3 in the gold at the outer boundary.

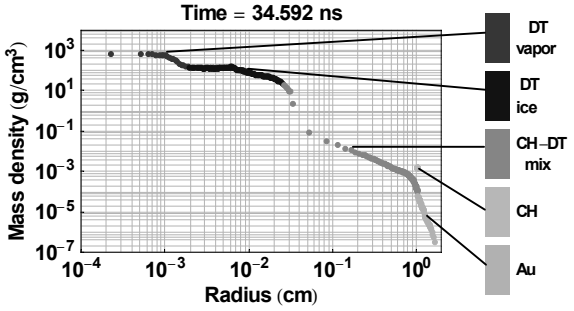

Fig. 4. Target mass density profile at 34.592 ns. Each dot characterizes a Lagrangian constant-mass zone.

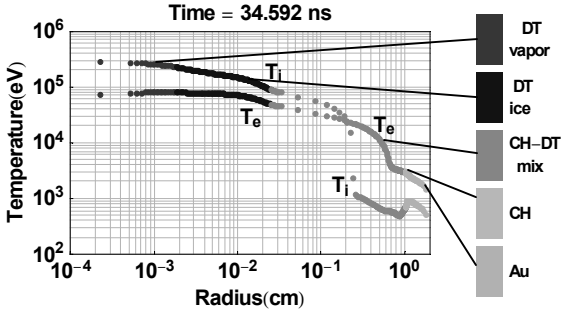

Fig. 5. Target ion and electron temperature profiles at 34.592 ns.

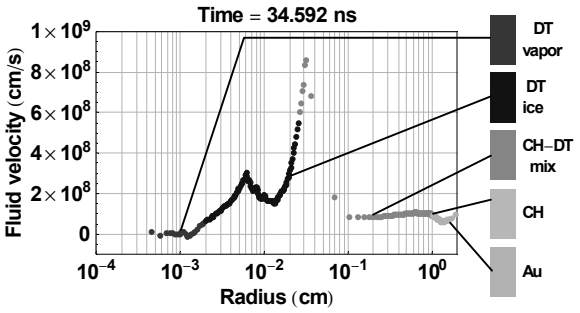

Fig. 6. Fluid element velocities vs. radius at 34.592 ns.

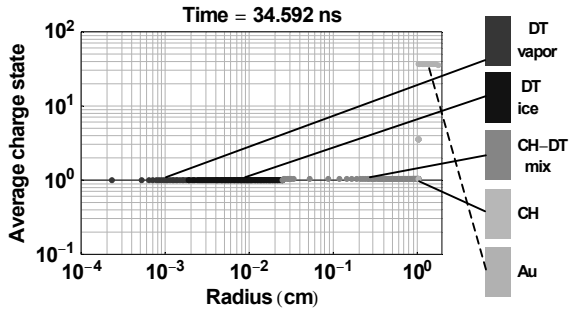

Fig. 7. Average charge state vs. radius for each Lagrangian zone at 34.592 ns.

III. SIMPLE MODEL PROBLEMS

Studying the fundamental dynamics of target expansion with the complexities of a full feature target using a multi-physics radiation hydrodynamics code such as BUCKY[2] is difficult. Certainly all relevant physics should be included but particular features are better understood using simpler models.

III.A. Expansion Cooling of Ionic Debris

A simple estimate of expansion cooling makes the point that even extremely high temperature dense plasma cools to low temperature upon expanding into a vacuum. Assume an initial plasma temperature of 50 keV and enclosing radius of 0.1 cm. Isentropic expansion of this plasma from a radius of 0.1 cm to a radius of 600 cm results in a final temperature of 16 K (assuming it behaves like a gamma law gas with γ=5/3). This is clearly a nonsensical result. A more interesting result is the radius of expansion corresponding to a temperature of 1000 K which might be typical of a first wall temperature in an IFE reactor chamber. This radius is r=76 cm. Thus a plasma expansion of less than a meter reduces the plasma temperature to the ambient temperature of the target chamber. Within the hydrodynamic description, the internal energy of the plasma, represented by the plasma temperature, approaches zero and all energy is converted to fluid kinetic energy of the outward expanding plasma.

III.B. Shock Propagation Down a Density Gradient

Another question to ask is: can plasma ions be accelerated to fluid energies that are greater than the energy associated with the initial energy density? That is, can the initial energy density be concentrated in a smaller mass of plasma and thus create a higher temperature? In fact the initial energy density can theoretically be concentrated in a smaller mass of plasma by a shock wave propagating down a density gradient.[3] As the density tends toward zero and the shock width remains the same, the resultant temperature behind the shock tends to infinity. This is governed by the formula in equation (1) that is valid for the power law density planar geometry profile given in equation (2).[4]

$$T \sim |\dot{X}|^2 \sim X^{\frac{-2(1-\alpha)}{\alpha}} \qquad (1)$$

$$\rho = bx^{\delta} \qquad (2)$$

In this case $\dot{X}$ is the shock front velocity and x is the spatial position variable. For γ=5/3 and δ=13/4 the value of α is α=0.59. [These values are taken from Ref. 4 and are typical of stellar atmosphere conditions for which this analysis was first performed. In fact it was postulated that this phenomena was responsible for very high energy cosmic radiation.[5]] Of course the shock front does not lead to infinite temperature as energy is compressed into smaller mass at the surface of this model mathematical problem. In fact, kinetic effects influence the result. The shock wave reaches a point in the density gradient where the ion mean free path is comparable to the shock thickness and classical fluid dynamics no longer accurately describes the processes. We next look at these kinetic effects and estimate their influence on shocks in the range of parameters found in our exploding target.

IV. KINETIC EFFECTS ON THE SHOCK

The main ions of concern for the present analysis are cold ions that, in the shock frame, have mean free paths longer than the shock thickness. When that situation occurs, the maximum energy an ion can reach will be limited. The BUCKY radiation hydrodynamics code[2] predicts that the velocity of the primary shock wave at ignition is ~6x10^8 cm/s, after which it slowly rises to ~10^9 cm/s, as shown in Fig. 8. Several shocks typically

occur simultaneously, because of the different masses and species in different regions, as can be seen in the r-t plot for the critical time interval of 30-40 ns in Fig. 9.

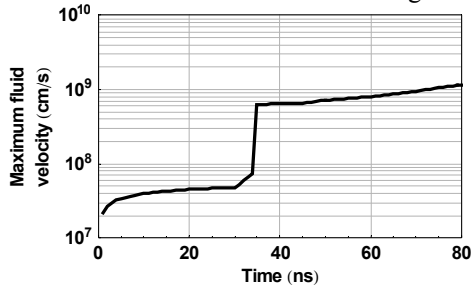

Fig. 8. Maximum fluid velocity (shock velocity) vs. time.

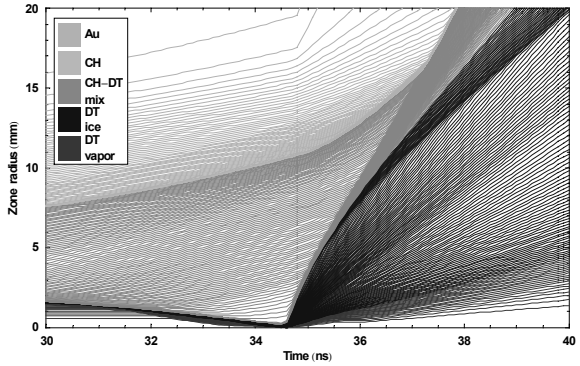

Fig. 9. Lagrangian zone radii vs. time between 30 and 40 ns, when most of the shock wave interactions occur.

The plasma parameters at 34.592 ns, shortly after ignition, will be used here to illustrate the impact of kinetic effects (long mean free paths) on ion energies. At 34.592 ns, shock waves are occurring in the CH-DT interface zones just outside of the pure DT zones and the zones at the interface where the plastic impacts the gold. The key parameters for these shocks and for the dense core inside r = 6 μm are given in Table I and Table II. The corresponding mass density, ion and electron temperatures, fluid velocity, and charge state for each zone were given in Fig. 4, Fig. 5, Fig. 6, and Fig. 7.

Combining the shock velocity with the average density, temperature, and charge state within the shock allows the calculation of the mean free path of the relatively cold ions as they pass through the shock wave. In the shock frame, the background ions have the lab-frame shock velocity. The calculation of the mean free paths uses standard formulas,[6] and we use the mass densities of Fig. 4 and fluid velocities of Fig. 6 to define the shock thickness.

The maximum velocity change of a background ion will be $\Delta v = v_s\left[1-\exp(-\delta_s/\lambda)\right]$, where Δv is the energy change, δ_s is the shock thickness, and λ is the mean free path. The corresponding energy change will be $E = \frac{1}{2} m_i (\Delta v)^2$, where m_i is the ion's mass.

Table I. Key parameters for the dense core at 34.592 ns.

	DT Core
Mass density, g/cm^3	600
Ion number density, cm^{-3}	1.5 x 10^{26}
Ion temperature, keV	276
Electron temperature, keV	72
Ave. charge state	1.0 / 1.0
Velocity, cm/s	6.6 x 10^4
Core radius, μm	50
Mean free path, nm	< 1

Table II. Key parameters for the shocks at 34.592 ns.

	DT/CH Shock	**CH/Au Shock**
Approx. radial position, cm	0.026	1.1
Velocity, cm/s	5.5 x 10^8	8.6 x 10^7
Effective ion energy, keV	388 keV	25
Mass density, g/cm^3	21	0.0016
Ion number density, cm^{-3}	5.1 x 10^{24}	5.0 x 10^{18}
Ion temperature, keV	86	2.8
Electron temperature, keV	47	0.69
Ave. charge state	1.0 / 1.0	1.0 / 36
Shock thickness, cm	0.002	0.004
Mean free path, cm	0.0018	4.0
Velocity change, cm/s	3.6 x 10^6	8.5 x 10^4
Energy change, keV	173	~0

In the core at 34.592 ns, the expansion velocity is modest and the density is very large. The highest density part of the core at this time has a radius of ~0.001 cm and a mass density of ~600 g/cm^3. The mean free paths are very short for almost all ions on which the expanding plasma impinges and the fluid approximation works well.

At 34.592 ns, the main shock at 0.02 cm < r < 0.04 cm (see Fig. 6) passes through the background CH ions, and the mean free path in the shock frame for slowing down of CH ions on the shock DT ions and electrons is 0.018 cm. This is approximately equal to the shock thickness of ~0.02 cm. The background ions, therefore, pick up only about two-thirds of the velocity and half of the energy from the passing shock wave that they would receive if the transfer were perfect. The shock thickness where the CH ions impact the Au ions, on the

other hand, is nearly 1000 times smaller than the mean free path at this time, primarily because the density at this radius has fallen by a factor of 10^6.

V. CONCLUSIONS

The overall conclusion of this paper is that conventional radiation hydrodynamics simulations of post-burn direct drive IFE target expansion are inadequate to model the ion spectrum. Comparison of shock thicknesses with ion-ion collision mean free paths for plasma parameters typical of such post-burn conditions show that the ion-ion mean free path is significantly larger than the shock thickness at a radius that is far interior to the target expanding surface. This invalidates the predicted shock acceleration of ions in the low density plasma beyond this radius. Further analysis must be done to fully characterize the differences between hydrodynamically predicted ion spectra and the true spectra. Empirical inclusion of kinetic effects in a conventional radiation hydrodynamics code is a practical approach that we are taking to improve predictions of ion threat spectra.

ACKNOWLEDGMENTS

This work was performed under the sponsorship of the High Average Power Laser Program under contract number N00173-03-1-G901.

REFERENCES

[1] J.D. SETHIAN, M. FRIEDMAN, R.H. LEHMBERG, M. MYERS, S.P. OBENSCHAIN, J. GIULIANI, P. KEPPLE, A.J. SCHMITT, D. COLOMBANT, J. GARDNER, F. HEGELER, M. WOLFORD, S.B. SWANEKAMP, D. WEIDENHEIMER, D. WELCH, D. ROSE, S. PAYNE, C. BIBEAU, A. BARAYMIAN, R. BEACH, K. SCHAFFERS, B. FREITAS, K. SKULINA, W. MEIER, J. LATKOWSKI, L.J. PERKINS, D. GOODIN, R. PETZOLDT, E. STEPHENS, F. NAJMABADI, M. TILLACK, R. RAFFRAY, Z. DRAGOJLOVIC, D. HAYNES, R. PETERSON, G. KULCINSKI, J. HOFFER, D. GELLER, D. SCHROEN, J. STREIT, C. OLSON, T. TANAKA, T. RENK, G. ROCHAU, L. SNEAD, N. GHONEIM, and G. LUCAS, "Fusion Energy with Lasers, Direct Drive Targets, and Dry Wall Chambers," *Nucl. Fusion* **43**, 1693 (2003).

[2] R.R. PETERSON, D.A. HAYNES, I.E. GOLOVKIN, and G.A. MOSES, "Inertial Fusion Energy Target Output and Chamber Response: Calculations and Experiments," *Phys. Plasmas* **9**, 2287 (2002).

[3] Y.B. ZEL'DOVICH and Y.P. RAIZER, *Physics of Shock Waves and High-Temperature Hydrodynamic Phenomena, Vol II*., Academic Press, New York, 1967, p. 812.

[4] G.M. GANDEL'MAN and D.A. FRANK-KAMENETSKII, "Shock Wave Emergence at a Stellar Surface," *Soviet Phys. `Doklady'* (English transl.) **1**, 223 (1956).

[5] S.A. COLGATE and M.H. JOHNSON, "Hydrodynamic Origin of Cosmic Rays," *Phys. Rev. Lett*. **5**, 235 (1960).

[6] J.D. HUBA, *NRL Plasma Formulary*, Naval Research Laboratory Report NRL/PU/6790-00-426 (2000).